Enhanced Particle Filter and Cyclic Spectral Coherence based Prognostics of Rolling Element Bearings

Junyu Qi[1], Alexandre Mauricio[2], Mathieu Sarrazin[3], Karl Janssens[4], and Konstantinos Gryllias[5]

[1,2,5]Division PMA, Department of Mechanical Engineering, Faculty of Engineering Science, KU Leuven, Dynamics of Mechanical and Mechatronic Systems, Flanders Make, *Celestijnenlaan 300, BOX 2420, 3001 Leuven, Belgium*

junyu.qi@kuleuven.be
alex.ricardomauricio@kuleuven.be
konstantinos.gryllias@kuleuven.be

[3,4]Siemens Industry Software NV, Leuven, Belgium

mathieu.sarrazin@siemens.com
karl.janssens@siemens.com

ABSTRACT

In the era of Internet of Things and Industry 4.0, the demand for condition monitoring of rotating machinery in industry becomes ever more significant. In addition to the steps of fault detection and diagnosis, the accurate estimation of the Remaining Useful Life (RUL) of machinery components may provide significant economic merits, optimizing the maintenance and avoiding potential human casualties and environmental pollution. During the last decades, a number of methodologies have been developed in the area of Prognostics and Health Management (PHM), categorized mainly in three groups, the physics based, the data-driven and the hybrid approach groups. Physical models are related to the load, the speed, the material, the geometry, etc. of a specific component and are able to make accurate RUL predictions but at an expensive computation cost and high complexity. In order to facilitate the applicability, a number of data-driven methodologies have been proposed including various versions of Kalman and Particle Filters. Among others, the Bayesian inference based Particle Filter provides high prediction accuracy for complex nonlinear systems utilizing little amount of data compared to machine learning techniques. The Monte Carlo step of the method is optimal to deal with the stochastic degradation process of bearings and appears to be able to handle any form of noise distribution. However, the traditional resampling methods frequently present the problem of particle leanness which heavily influences the performance of PF. The existing prediction methodologies are mainly based on classical diagnostic features, e.g. RMS, reaching a limit of efficacy. In order to overcome the abovementioned bottlenecks, an advanced prognostic methodology is proposed based on PF, the systematic resampling method and the Cyclic Spectral Coherence (CSCoh). The systematic resampling is proposed in order to address the problem of impoverishment. Moreover the CSCoh has been recently proposed as a powerful tool revealing weak modulations masked in the signals. The integration of the CSCoh over the frequency leads to the Enhanced Envelope Spectrum and a diagnostic feature is estimated based on the sum of the amplitudes of three harmonics of the characteristic fault frequencies of rolling element bearings. The methodology is tested and evaluated on experimental vibration signals, while the performance is quantitatively evaluated using prognostic metrics in the consideration of accuracy, precision and convergence.

1. INTRODUCTION

In the era of Industry 4.0 (Ferreiro et al. 2016), Condition Monitoring (CM) is attracting significant industrial attention. On one hand, the obtained CM information reflects the operation status of machinery and helps to identify the existing faults, reducing further the breakdown time and avoiding severe economic loss. On the other hand, due to the development of sensor technology and advanced computation power, large amount of data of production processes are able to be collected, which ranges from the level of single machine component to the system. Moreover, the analysis of the gathered data contributes to the optimization of the production. In the last several decades, the application of CM was mainly focused on the level of fault detection and diagnosis. Today, predictive maintenance is widespread discussed and integrated into the framework of Prognostics and Health Management (PHM). Prognostics allows for the estimation of the Remaining Useful Life (RUL) of a component from the current time till the End Of Life

(EOL). Therefore, proactive actions such as specific maintenance planning (ordering and preparation of components etc.) are able to be scheduled beforehand.

Rolling Element Bearings (REBs) are frequently utilized in machines in order to transfer relative movements and forces. REBs often lead to machine breakdowns and as a result the prediction of the RUL of REBs plays a significant role in the CM of equipment. The state of art can be mainly categorized into three groups, the data-driven, the physics-based and the hybrid approach. The physics-based approach requires extensive knowledge about the failure mechanism and is related generally with a number of factors (Bolander et al. 2016) such as the fault type, the material, the geometry properties, the speed and the load. The Paris law and the Forman law are typical physical models, indicating the rate of crack growth and have been broadly studied. A reliable physics model achieves more accurate performance, however, its configuration is often designed for a specific fault type and application. Therefore, the data-driven methods have been proposed with the merit of flexibility. An approximation model is directly estimated from the experimental data, without the necessity of complex modeling. Wu et al. (2016) classified the data driven methods in the Machine Learning methods (ANN, Deep Learning, etc.), the Filter methods (Kalman Filter, Particle Filter) and the Stochastic Process methods (Gaussian, Wiener). In addition, the hybrid approach, combining data-driven and physics models, could be a beneficial choice in the view of reliability and accuracy. However, under the consideration of applicability, the data-driven approach is becoming the mainstream nowadays and the prediction performance is improved gradually as well.

In the case of highly nonlinear systems, the Particle Filter (PF) methods have great potential value in comparison to others in the aspect of the data amount, the accuracy and the computation cost. Li et al. (2017) investigated the RUL prediction of bearings based on a new PF (combined with Genetic algorithms) and a time varying autoregressive model. The performance of PF is more accurate than a Support Vector Machine based prognostics method using the RMS and the Peak Value as features. Deutsch et al. (2017) selected RMS as feature and fused the PF with deep learning in order to estimate the RUL. Li et al. (2015) proposed an exponential degradation model for the PF and studied the selection of the first prediction point using the features of RMS and Kurtosis. The proposed approach demonstrated interesting results based on the validation data. Qian et al. (2015) enhanced the PF with a back propagation neural network and used RP entropy as a feature leading to a prediction superior to a Support Vector Regression.

However, a number of issues are still confronted and worth more exploration in the current framework, e.g. the decision of the start prediction point, the threshold setting to the EOL, the parameters tuning, the particle degeneracy, the decision of particle number, the data model selection, etc. Taking into consideration the existing bottlenecks, this work presents a methodology for the estimation of the RUL of REBs based on the Enhanced Particle Filter and the Enhanced Envelope Spectrum (EES), which is derived from the Cyclic Spectral Coherence (CSCoh) (Antoni, 2007). The rest of the paper is organized as follows. The theory of Particle Filter as well as the Systematic Resampling (Li et al., 2015) are explained in detail in section 2. Subsequently, an advanced monitoring feature based on the EES is introduced in section 3. Furthermore, a general REBs RUL estimation procedure based on Cyclostationary monitoring features and Enhanced Particle Filter is presented in section 4. Moreover, a number of performance metrics are presented in section 5 in order to evaluate quantitatively the results of the RUL estimation. The experimental data and the analysis of the prediction results are discussed respectively in section 6 and section 7. The paper is closing with some conclusions.

2. PARTICLE FILTER

As a typical type of Bayesian estimation method, Particle Filter (PF) uses a number of particles to estimate the posterior distribution of a stochastic process with random perturbation. In this section, the theory of Particle Filter and the Systematic Resampling are briefly presented.

2.1. Classic Particle Filter

The Classic Particle Filter (CPF) is particularly useful for the estimation of a nonlinear dynamic system with non-Gaussian noise. The principles of CPF is based on the Bayesian theory and different sampling methods, including the Monte Carlo Sampling (MCS), the Importance Sampling (IS), the Sequential Importance Sampling (SIS) and the Sequential Importance Resampling (SIR). Each of them is briefly explained as follows.

The Bayesian theory includes prediction and update steps. In the prediction step, the priori Probability Density Function (PDF) of the k_{th} predicted state x_k is expressed with the help of the posteriori knowledge (the measurements $z_{1:k-1}$), that is $p(x_k|z_{1:k-1})$. Afterwards, the posteriori PDF $p(x_k|z_{1:k})$ is updated when the k_{th} measurement z_k is available.

According to the logic of MCS, the state x_k is approximated by a set of particles $x_k^i, i = 1 \dots N$, which are sampled from a certain probability distribution. The posteriori probability of Bayesian estimation is able to be approximated with MCS, $p(x_k|z_{1:k}) \approx \frac{1}{N} \sum_{i=1}^{N} \delta(x_k - x_k^i)$, where δ denotes the Dirac delta function. Each particle has the same weight $\frac{1}{N}$.

In order to overcome the limitation of the normal distribution assumption of MCS the IS has been proposed. The posteriori PDF can be rewritten as

$$p(x_k|z_{1:k}) = \frac{p(x_k|z_{1:k})}{q(x_k|z_{1:k})} q(x_k|z_{1:k})$$

$$= \frac{p(z_{1:k}|x_k)p(x_k)}{p(z_{1:k})q(x_k|z_{1:k})} \cdot q(x_k|z_{1:k})$$

$$= \frac{w_k(x_k)}{p(z_{1:k})} \cdot q(x_k|z_{1:k})$$

$$= \frac{w_k(x_k) \cdot q(x_k|z_{1:k})}{\int w_k(x_k) \cdot q(x_k|z_{1:k})dx_k}$$

$$= \frac{\widetilde{w}_k(x_k)}{\int \widetilde{w}_k(x_k)dx_k} \tag{1}$$

where,

$$w_k(x_k) = \frac{p(z_{1:k}|x_k)p(x_k)}{q(x_k|z_{1:k})} \propto \frac{p(x_k|z_{1:k})}{q(x_k|z_{1:k})} \tag{2}$$

Therefore, the N particles are sampled from the importance distribution $q(x_k|z_{1:k})$, and the corresponding weights are normalized following Eq. (3):

$$\widecheck{w}_k(x_k^i) = \frac{\widetilde{w}_k(x_k^i)}{\sum_{i=1}^{N} \widetilde{w}_k(x_k^i)} \tag{3}$$

The recursive equation of the particles weights for $q(x_{0:k}|z_{1:k})$ is thus written as:

$$w_k^i \propto \frac{p(x_{0:k}^i|z_{1:k})}{q(x_{0:k}^i|z_{1:k})} = w_{k-1}^i \frac{p(z_k|x_k^i)p(x_k^i|x_{k-1}^i)}{q(x_k^i|x_{0:k-1}^i, z_{1:k})} \tag{4}$$

The importance distribution $q(x_k|x_{0:k-1}, z_{1:k})$ in Eq. (4) is related with all the previous measurements and results in heavy computation cost for each measurement. In order to reduce the computation time SIS has been proposed and the q is assumed to be dependent only on the previous state x_{k-1} and the current measurement z_k. Then, the weight calculation of Eq. (4) is transformed as:

$$w_k^i \propto w_{k-1}^i \frac{p(z_k|x_k^i)p(x_k^i|x_{k-1}^i)}{q(x_k^i|x_{k-1}^i, z_k)} \tag{5}$$

However, the main issue of SIS lies in the problem of particles degeneracy. The number of 'effective' particles decreases after some certain recursive steps and, in other words, the weight of the most particles becomes negligible. Hence, the resampling duplicates the high weight particles and replaces the lower ones. The importance distribution $q(x_k|x_{k-1}, z_k)$ is generally chosen as $p(x_k^i|x_{k-1}^i)$, and then $w_k^i \propto w_{k-1}^i p(z_k|x_k^i)$.

Based on the abovementioned background, CPF mainly consists of three steps, the particles generation, the weight calculation and the resampling.

1. Particles generation

As an initial step, the amount (N) of particles are firstly generated from a priori distribution and pass further through the transition model, $x_k^i \sim p(x_k|x_{k-1}^i), i = 1 \dots N$.

2. Weight calculation

The likelihood of each particle x_k^i is calculated with the available measurement z_k, $w_k^i = p(z_k|x_k^i)$, and then is normalized as $\widecheck{w}_k^i = \frac{w_k^i}{\sum_{i=1}^{N} w_k^i}$.

3. Resampling

In the most frequently used resampling method (the multinomial resampling), the weight of each particle is measured with a threshold, which is selected as a random value between 0 and 1. Only the particles with high weight (above threshold) are kept.

2.2. Enhanced Particle Filter

The procedure of Enhanced Particle Filter (EPF) is similar to CPF and consists of three steps as well: a) the particle generation, b) the weight calculation and c) the resampling.

In this work, the Systematic Resampling (SR) is utilized to replace the resampling step of CPF and enhance the performance. Unlike the traditional method, which is implemented for the whole interval U with a random threshold between 0 and 1, the SR divides the whole interval into N subspaces $U^i = \left(\frac{i-1}{N}, \frac{i}{N}\right), i = 1, \dots, N$, and the particles are taken with a corresponding random threshold in the U^i.

In comparison with the traditional approach, the principle of SR guarantees more particle diversity in each recursive step and additionally the computation complexity for the U^i is lower than for the original U (Li et al. 2015). Therefore, SR is combined with step 1 and 2 presented in CPF and is considered as an enhanced version of the Particle Filter.

3. CYCLIC SPECTRAL COHERENCE

Cyclostationary signals are a special category of nonstationary signals carrying hidden periodicities in their structure. A signal is characterized as first order cyclostationary (CS1) if its first order statistical moment is a periodic function of period T.

$$M_{1x}(t) = E\{x(t)\} = M_{1x}(t + T) \tag{6}$$

The second-order of cyclostationarity (CS2) can be defined as a function whose autocorrelation is T-periodic:

$$R_{2x}(t, \tau) = R_{2x}(t + T, \tau) = E\{x(t)x^*(t - \tau)\} \tag{7}$$

where t represents the time, x stands for the vibration signal, τ is the time lag and E is the ensemble average operator. The Cyclic Spectral Correlation (CSC) can be firstly estimated, describing the pair of frequency shifted correlations.

$$S_x(\alpha, f) = \lim_{W \to \infty} W^{-1} E[\mathcal{F}^W\{x(t)\}^* \mathcal{F}^W\{x(t)\}] \tag{8}$$

where, W is the time duration and $\mathcal{F}^W\{x(t)\}$ is the Fourier transform of signal $x(t)$. The processing of the CSC reveals

the correlation levels at which each carrier frequency f is modulated by the cyclic frequency α.

The Cyclic Spectral Coherence (CSCoh) is defined (Antoni, 2007) as the normalization of the Cyclic Spectral Correlation:

$$\gamma(\alpha, f) = \frac{S_X(\alpha, f)}{\sqrt{S_X(0, f) S_X(0, f - \alpha)}} \tag{9}$$

The CSCoh takes values in the range between 0 and 1. The CSCoh can be presented as a map in the plane of the frequency f and the cyclic frequency α. The integration of the CSCoh over the carrier frequency axis f has been proposed in order to extract a spectrum termed as Enhanced Envelope Spectrum (EES), which is an improved version of the classical Squared Envelope Spectrum:

$$EES(\alpha) = \frac{1}{f_2 - f_1} \int_{f_1}^{f_2} |\gamma(\alpha, f)| df \tag{10}$$

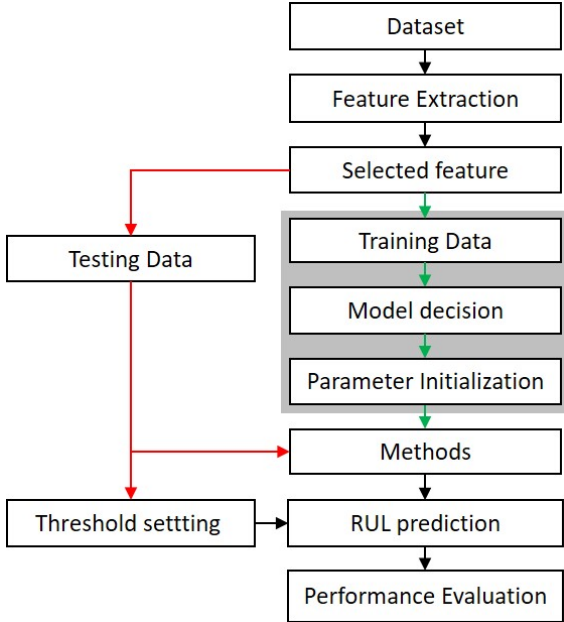where f_1 is equal to zero and f_2 is equal to the Nyquist frequency.

Figure 1. Flowchart of the RUL prediction.

4. METHODOLOGY FOR THE ESTIMATION OF THE REMAINING USEFUL LIFE OF REBS

In this paper an advanced data driven methodology for the estimation of the RUL of rolling element bearings is presented based on the Enhanced Particle Filtering and the Enhanced Envelope Spectrum. The proposed general methodology consists of different steps as presented in the Flowchart in Figure 1.

Step 1: Loading of Dataset

The methodology is based on the exploitation of available training data, e.g. available field data or data captured during an accelerated degradation test.

Step 2: Feature extraction

Different signal processing techniques can be used in order to extract dedicated diagnostic/prognostic features in the time, frequency, time-frequency or frequency-frequency domain.

Step 3: Feature selection

The prognostic feature should follow accurately the degradation process. The goodness of the feature can be characterized by three aspects: the monotonicity, the prognosability and the trendability. Additionally, the diagnostic/prognostic feature should detect the fault at an early stage in order to facilitate the early start of prediction. Recently, the EES based on the CSCoh has been proposed as a powerful technique in the fault diagnosis (Antoni 2007, Ricardo Mauricio et al. 2018) and a CSCoh based feature is therefore introduced in this paper. The feature is defined as the sum of the M-harmonics of the characteristic bearing fault frequencies f_{fault}.

$$y = \sum_{j=1}^{M} EES(j\, f_{fault}) \tag{11}$$

where $EES(j\, f_{fault})$ indicates the amplitude of the j_{th} harmonic of the characteristic fault frequency. In this paper M=3 harmonics are considered. The feature is further smoothed in order to remove possible outliers and fluctuations.

Step 4: Setting fault detection and End Of Life Thresholds
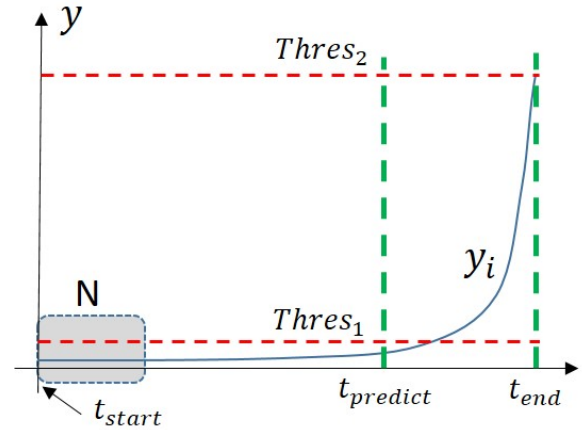

Figure 2. Illustration of threshold decision.

As demonstrated at Figure 2, the monitoring feature is expected to have a stable trend in the beginning. The average value of the first N samples is consider as the health reference H_0:

$$H_0 = \frac{1}{N} \sum_{i=1}^{N} y_i \tag{12}$$

The start time of prediction $t_{predict}$ is triggered by H_0 when the feature value exceeds a threshold $Thres_1$.

$$Thres_1 = (1 + perc) \cdot H_0 \tag{13}$$

The percentage $perc$ can be defined based on the experience specifically for each case. The second threshold $thres_2$ corresponds to the End Of Life (EOL) of the bearing/component.

$$Thres_2 = y_{end} \qquad (14)$$

Therefore, the samples below the $Thres_1$ are utilized as training data, and the rest between $Thres_1$ and $Thres_2$ as testing data.

Step 5: Data model decision

A degradation data model is selected corresponding to the selected feature. The model $f(a_1, a_2, \ldots, a_n)$, characterized by the model parameters $a_1, a_2, \ldots, a_n$ should describe well the monitoring feature.

Step 6: The initial parameters

The initial parameters $a_{10}, a_{20}, \ldots, a_{n0}$ of the model can be extracted using curve fitting on the training data. Moreover the Particle Filter requires the initially manual selection of the corresponding variance of the parameters, i.e. the $Q_{a1}, Q_{a2}, \ldots, Q_{an}$, the process noise variance Q_x and the measurement noise Q_z. The particle number is also an influence factor, which could be further evaluated in terms of the estimation accuracy, the computation effort and the efficient particle rate.

Step 7: Particle Filter

As the key part of the proposed framework, the selected model is adopted as the transition equation of a PF and is initialized with the fitted parameters. In this paper an Enhanced Particle Filter is used based on the Systematic Resampling approach, which allows the update of the model parameters at each step as soon as a new measurement is available by calculating the likelihood.

Step 8: RUL prediction

The RUL is calculated based on the Eq. (15) and (16):

$$f(a_{1k}, a_{2k}, \ldots, a_{nk}, t_k) = Thres_2 \qquad (15)$$

where, $a_{1k}, a_{2k}, \ldots, a_{nk}$ are the model parameters at the k_{th} step. Finally the RUL can be estimated as:

$$RUL_k = t_k - k \qquad (16)$$

As the bearing degradation evolves stochastically, the RUL prediction should not be provided by only a single value but be accompanied by a Confidence Interval (CI). The upper and the lower bound of the CI can be calculated as:

$$x_{upper} = \bar{x} + z^* \frac{\sigma}{\sqrt{n}} \qquad (17)$$

$$x_{lower} = \bar{x} - z^* \frac{\sigma}{\sqrt{n}} \qquad (18)$$

where, $\bar{x}$ indicates the predicted mean value, σ the standard deviation of the amount n particles and z^* stands for the critical factor, which is selected equal to 1.96 for 95% of CI.

Step 9: Evaluation

The performance of the methodology can be evaluated using a number of performance metrics which are presented in section 5.

5. PERFORMANCE METRICS

In order to evaluate the quality of the prediction results, a number of performance metrics, presented at Table 1, can be used.

Table 1. Performance metrics.

Metrics	Formula	PS
AC	$\frac{1}{N} \sum_{i=1}^{N} e^{-\frac{|error|^\alpha}{Re(i)}}$	1
PR	$\sqrt{\frac{\sum_{i=1}^{N}(error(i) - \overline{error})}{N}}$	0
PH	$Pr(i) \epsilon [Re(i)(1 - \alpha_c), Re(i)(1 + \alpha_c)]$	N
MAE	$\frac{1}{N} \sum_{i=1}^{N} |error(i)|$	0
ERR	$\frac{|100 \cdot error(N)|}{Re(N)}$	0

The coefficients α and α_c inside the formula of AC and HP should fulfill the conditions that $\alpha \in [1, 2]$ and $\alpha_c \in [0, 100]\%$ and are selected equal to 1 and 20% respectively in this paper.

Five criteria have been utilized in order to evaluate quantifically the results in the view of accuracy and precision. Precision (PR) is a measurement of the dispersion of the prediction error, while the others evaluate the error itself. Accuracy (AC) expresses the relative error in percentage. Prognostics Horizon (PH) counts the number of prediction points falling within the error bound ($\pm\alpha_c = \pm20\%$) regarding to the actual RUL. The Mean Absolute Error (MAE) describes the average of the absolute error while the Error (ERR) indicates the error of the final point, representing the convergence of the final prediction. In the end, the achieved performance value is compared with the Perfect Score (PS), which signifies the ideal prediction.

6. EXPERIMENTAL SETUP – DATA DESCRIPTION

The proposed methodology is validated and evaluated on the Intelligent Maintenance Systems (IMS) public domain dataset. The experimental data has been captured during an endurance test realized at University of Cincinnati (Qiu et al. 2009). The test rig consists of an electric motor, a pulley system and a shaft mounted on four double row Rexnord ZA-2115 bearings (Figure 3). A radial load is applied on bearings No 2 and 3. The bearings are tested under constant operation

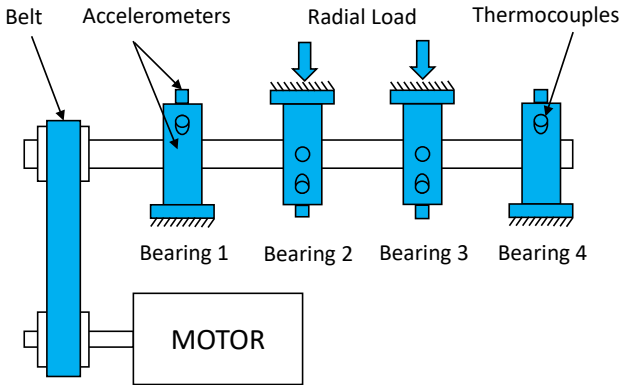conditions (rotating speed $n = 2000\ rpm$, radial load $F = 6000\ lbs$).

Figure 3. Experimental setup and sensor placement.

Three run-to-failure datasets have been collected. The End Of Life (EOL) of the bearings has been defined as a certain Accumulated Debris Level (ADL) on the magnetic plug. The detailed information about the experimental setup and the corresponding bearings and sensor locations is illustrated at Figure 3.

Table 2. Characteristics of bearings.

Physical Parameters	
Pitch diameter	71.5 mm
Rolling element diameter	8.4 mm
Number of rolling element per row	16
Contact angle	15.7°
Static load	26690 N
Characteristic Frequencies	
Shaft frequency	33 Hz
Ball Pass Frequency Outer Race (BPFO)	236 Hz
Ball Pass Frequency Inner Race (BPFI)	297 Hz
Ball Spin Frequency (BSF)	278 Hz
Fundamental Train Frequency (FTF)	15 Hz

Two accelerometers were attached on the bearing mountings in the x and y direction during the 1st dataset while only one direction was used for the 2nd and 3rd dataset. The duration of each signal is equal to one (1) second and sequential measurements were captured every 10 minutes using a NI DAQ Card 6062E. The sampling frequency f_s has been reported as 20 kHz but it seems that it had been set equal to 20.48 kHz. The physical parameters and the characteristic frequencies of the REBs under the specific operation condition are listed in Table 2. At the end of the 1st endurance test, a defect was identified at the inner race of bearing No 3 and at the rolling element of bearing No 4. An outer race defect on bearing No 1 and an outer race defect on bearing No 3 have been respectively identified at the end of the second and the third test. In this paper, the signals captured on the bearing No 3 of test 1 and on bearing No 1 of test 2 are processed.

7. RESULTS AND DISCUSSION

The abovementioned methodology for the estimation of the RUL is applied, tested and evaluated using the experimental data described above.

7.1. CSCoh based Feature

The feature extraction method presented in section 3 has been applied on the signals of dataset 1 and dataset 2 and the diagnostic features (based on the BPFI and the BPFO respectively) are presented at Figure 4 and 5. The raw features present fluctuations and therefore a median smoothing filter with a filter length equal to 15 is applied. In the case of dataset 1, shown in Figure 4, a stable trend is identified before t = 1800 (x 10 min), which further increases and fluctuates slowly between 1800 (x 10 min) and 2000 (x 10 min). Next, the degradation evolves faster with a steeper increasing slope and heavy fluctuation. In the dataset 2, the fault can be identified around 528 (x 10 min) and the amplitude of the feature increases afterwards, fluctuates strongly from 700 (x 10 min) but remains around the value of 1.2 after 800 (x 10 min).
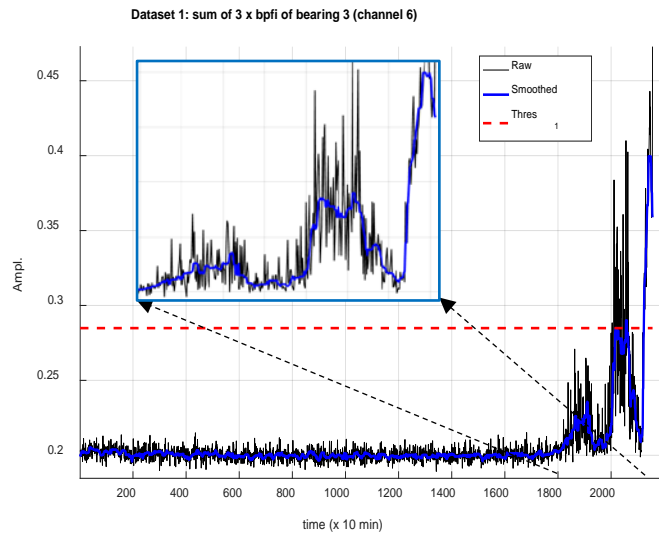

Figure 4. CSCoh based feature of dataset 1.

7.1.1. Threshold setting

Following the ideal trend presented in Figure 2, the features presented in Figure 4 and Figure 5 follow initially a stable trend. The first N points (N=100) are selected as healthy data and the value of $perc$ is selected equal to 40%. The corresponding threshold $Thres_1$ is marked with a red line at

the Figures 4 and 5. In general the threshold of EOL $Thres_2$ is set equal to the feature value of the last measurement, which ideally corresponds to the maximum value. However in the case of dataset 2, the $Thres_2$ is set equal to the maximum value which corresponds to the 980th measurements, as the feature presents a sudden significant drop at the end.
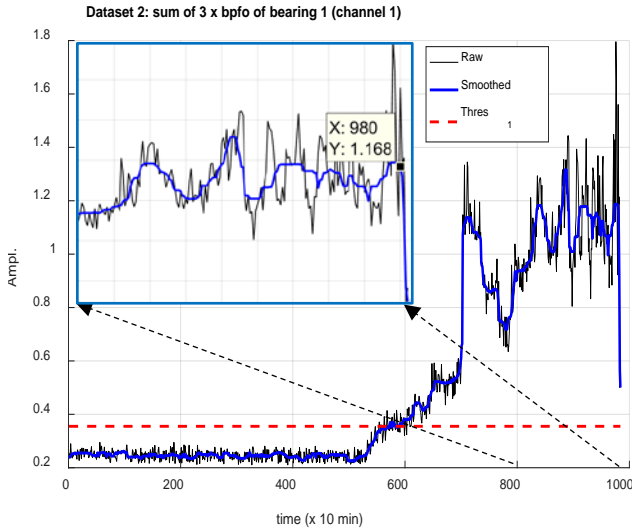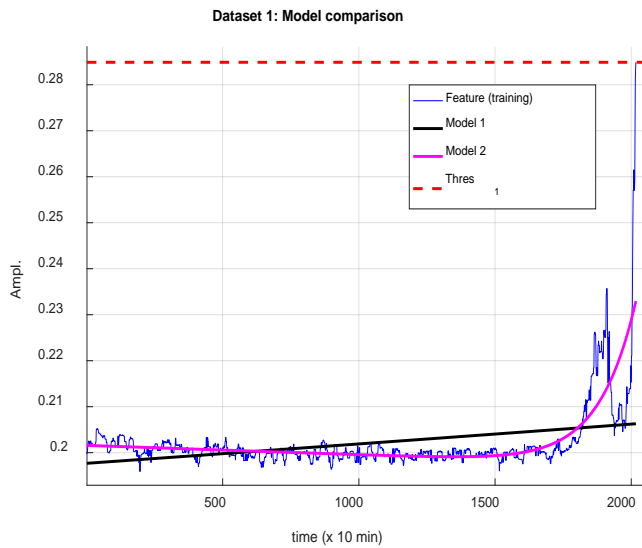

Figure 5. CSCoh based feature of dataset 2.

Figure 6. Model comparison for dataset 1.

7.1.2. Model selection

The data model plays a critical role in the PF and as a result the appropriate decision results in better initialization and representation of the monitoring feature. Thus, two candidate models, $f = ae^{b \cdot t}$ (model 1) and $f = ae^{b \cdot t} + ce^{d \cdot t}$ (model 2), are initially selected and quantitatively compared. The model is selected by minimizing the Mean Absolute

Percentage Error (MAPE) between the training feature line and the model. Model 2 presents a lower MAPE for both datasets as presented in Table 3 and tracks better the estimated feature as presented in Figure 6.

Table 3. MAPE of dataset 1 and 2.

	Model 1	Model 2
Dataset 1	1.7927	0.9850
Dataset 2	4.7027	2.7595

7.1.3. Initial parameters selection and parameter tuning

The model parameters a, b, c, d are initialized based on the model extracted by the training data. On the other hand the variances of Q_a, Q_b, Q_c, Q_d, the variance of the process noise Q_x and the measurement noise Q_z are selected manually. Moreover the number of particles should be selected. In order to evaluate the influence of the particle number and the resampling method, seven (7) particle numbers are selected (100, 300, 500, 1000, 2000, 5000 and 10000) and the results are compared in respect to the MSE (Figure 7) and the effective rate (Figure 8).
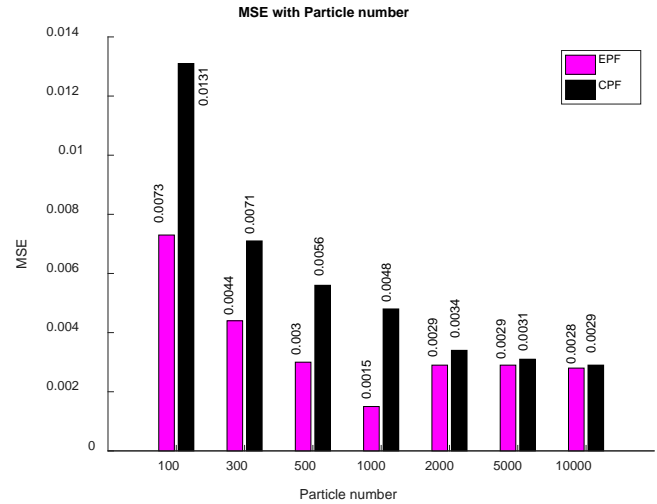

Figure 7. MSE for different particle number.

It can be noted that the increase of particle number leads to a decrease of the MSE both for the CPF and the EPF. In comparison to the CPF, the EPF presents a lower MSE in all cases. Moreover, the MSE in the EPF approach remains almost steady while the particle number increases significantly (>2000).

The effective rate of particles is presented in Figure 8. With the increase of the particle number, the efficient particle number increases fast for low amounts (<500) and then is stabilized. Compared to the CPF method, the EPF presents higher efficient particle numbers. Using the EPF, 500 particles are enough to reach the same effectiveness level

with 10000 particles which are needed in the case of CPF. Additionally the efficient particles rate for a high amount of particle number (>500) remains almost steady in the EPF. Therefore, the EPF achieves better performance compared to the classical PF. Based on the previous analysis the particle number is set equal to 500.
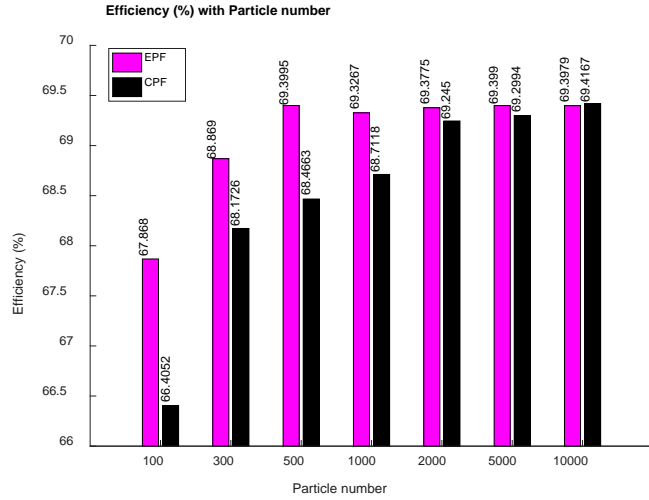

Figure 8. Efficiency for different particle numbers.

7.1.4. RUL prediction

Taking into account the chosen model, the RUL is estimated based on the following equations:

$$a_k \cdot e^{b_k \cdot t_k} + c_k \cdot e^{d_k \cdot t_k} = Thres_2 \tag{19}$$

where, a_k, b_k, c_k, d_k are the model parameters at the step k. The RUL is further estimated as:

$$RUL_k = t_k - k \tag{20}$$

7.2. Results of the RUL prediction

The methodology described above is further evaluated based on the two IMS datasets. The effectiveness of the estimation of the RUL using EPF is investigated and compared with CPF and other state of art methods, e.g. the simple extrapolation (EXT), the Classic Kalman Filter (CKF) and the Extended Kalman Filter (EKF). The EXT provides a RUL estimation using directly the model estimated based on the curve fit of real time data in each step. The performance of these methods are finally evaluated based on the abovementioned performance metrics.

7.2.1. Case 1: Bearing 3 of dataset 1

The feature estimation using the EXT, the CKF, the EKF, the CPF and the EPF is shown in Figure 9. Analyzing the figure, it can be concluded that the EXT, the CKF and the EKF provide a bad estimation of the feature value. The prediction based on the EPF achieves the best estimation. In order to quantitatively compare the performance of the three methods,

the error (MAPE) is estimated and as it can be seen in Table 4 the EPF achieves the best performance.

Table 4. MAPE of dataset 1.

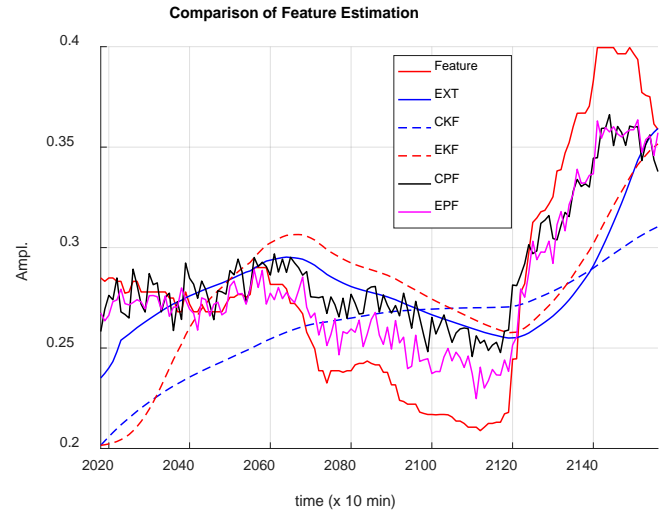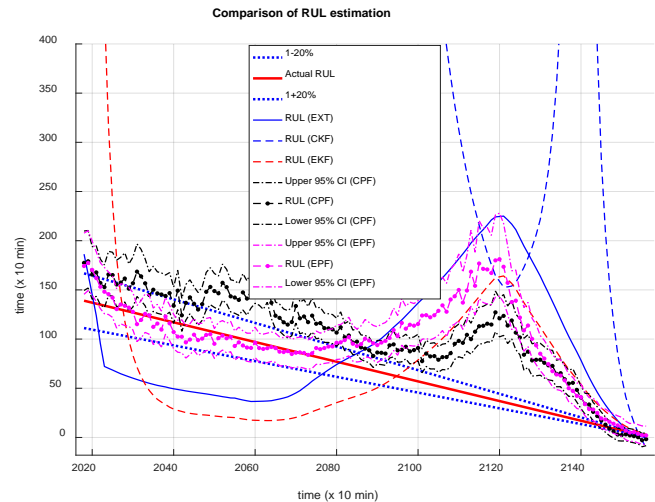| Method	MAPE
EXT	13.6
CKF	13.7
EKF	17.3
CPF	8.8
EPF	6.3

Figure 9. Feature estimation (Dataset 1).

Figure 10. RUL estimation (Dataset 1).

The performance of the RUL estimation is presented in Figure 10. The RUL estimated based on the CKF deviates significantly by the ("assumed") true one. The EXT, the EKF and the CPF predictions present a high error compared to the

EPF before the 2090 (x 10 min) and then approach the actual RUL till the 2147 (x 10 min). Afterwards the EXT and the CPF seem to underestimate the actual RUL as it can be seen in Figure 11. At the end the EPF provides a more accurate RUL prediction compared to all of others.
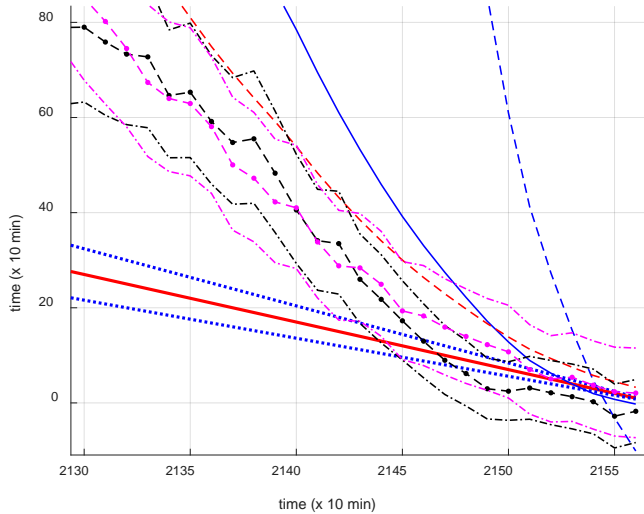

Figure 11. Zoom of the RUL estimation (Dataset 1).

In addition, the RUL prediction performance is also evaluated based on the performance metrics. The criterion of AC, HP, MAE and ERR note that EPF achieve the best results while the lower PR value of CPF indicates that the RUL prediction fluctuates less than others. Moreover, the MAE value (33.6) of EPF practically means that the RUL estimation presents a 5.6 hours difference for the predicted period (23.2 hours) while the HP (62) declares that 62 points fall into the error interval ($\pm 20\%$), which corresponds to around 10.3 hours.

Table 5. Performance metrics of Dataset 1.

	AC	PR	HP	MAE	ERR
EXT	0.4	82.6	12	69.7	125
CKF	0.4	7.7E4	0	2.5E4	110
EKF	0.4	232.5	8	96.7	-229
CPF	0.6	19.7	10	35	276
EPF	0.6	41.5	62	33.6	-107
PS	1	0	N	0	0

7.2.2. Case 2: Bearing 1 of dataset 2

Due to lack of space a figure demonstrating the feature estimation is not presented here but it should be noted that the EPF achieves the min error. The RUL of the bearing is predicted based on the three methods and the results are presented in Figure 12. The RUL estimated by the CKF and the EKF becomes negative after around 710 (x 10 min) and by the EXT after t = 840 (x 10 min). The RUL prediction based on the CPF fluctuates heavily at the beginning and then

decreases linearly presenting a bias from the actual RUL. However, the EPF seems to be the best method as most of its predicted RUL points fall within the error bound and starting from t = 600 (x 10 min) the RUL converges ideally to the straight line, still presenting a minor bias, as can be seen in the zoomed scope of Figure 12.
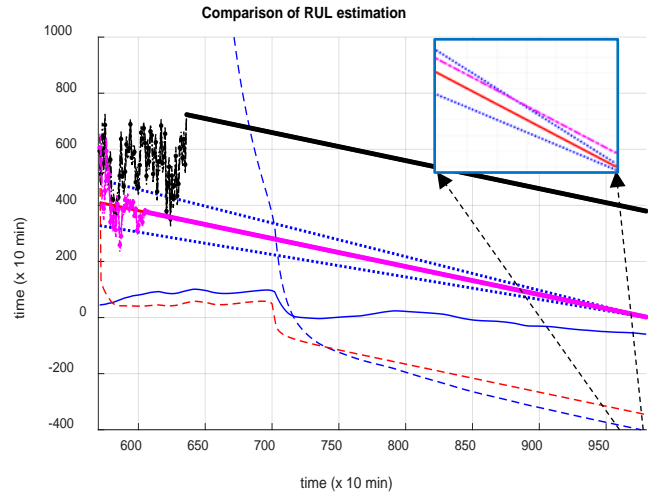

Figure 12. RUL estimation (Dataset 2).

The methods are further compared based on the prognostic metrics presented in Table 6. The EPF achieves the best performance based on all metrics. It could be mentioned that the value of MAE (5) indicates that there is only 0.835 hour error for the whole prediction period (68.3 hours).

Table 6. Performance metrics of Dataset 2.

	AC	PR	HP	MAE	ERR
EXT	0.4	75.5	0	185.5	6E3
CKF	0.1	2.7E4	3	5.8E3	4E4
EKF	0.2	42.2	0	328.9	4E4
CPF	0.2	85.1	10	345.2	-4E5
EPF	1	21	398	5	-88
PS	1	0	N	0	0

8. CONCLUSION

In this paper a prognostic methodology for the estimation of Remaining Useful Life of bearings exploiting the properties of Cyclic Spectral Coherence and the Particle Filtering have been presented. The different steps of the methodology have been analyzed and a guideline for the proper selection of the different parameters has been presented. An advanced resampling methodology is applied and its performance has been evaluated and compared with the classical one and other state of art approaches. Moreover the influence and the efficacy of the number of particles has been analyzed for two resampling approaches. Three different prediction methods have been evaluated and compared on the IMS dataset and

the Enhanced Particle Filter demonstrates the best performance based on performance metrics.

REFERENCES

Ferreiro, S., Konde, E., Fernandez S. & Prado, A. (2016), *Industry 4.0: Predictive Intelligent Maintenance for Production Equipment. Third European Conference of the Prognostics and Health Management Society.* July 6-8, Bilbao, Spain.

Bolander, N., Qiu, H., Eklund, N., Hindle, E & Rosenfeld, T. (2009), *Physics-based Remaining Useful Life Prediction for Aircraft Engine Bearing Prognosis. Annual Conference of the Prognostics and Health Management Society.* September 27- October 1, San Diego, CA.

Wu, L.F., Fu, X.H. & Guan, Y. (2016), *Review of the Remaining Useful Life Prognostics of Vehicle Lithium-Ion Batteries Using Data-Driven Methodologies. Appl. Sci.* 2016, 6, 166.

Li, K., Wu, J.J., Zhang, Q.J., Su, L. & Chen, P. (2017), *New Particle Filter Based on GA for Equipment Remaining Useful Life Prediction. Sensors (Basel, Switzerland).*

Deutsch, J., He, M. & He, D. (2017), *Remaining Useful Life Prediction of Hybrid Ceramic Bearings Using an Integrated Deep Learning and Particle Filter Approach. Appl. Sci.*, vol. 7(7), pp. 649.

Li, N.P., L., Y.G., Lin, J. & Ding S.X. (2015), *An Improved Exponential Model for Predicting Remaining Useful Life of Rolling Element Bearings. IEEE Transactions on Industrial Electronics*, vol. 62(12).

Qian, Y.N. & Yan, R.Q. (2015), *Remaining Useful Life Prediction of Rolling Bearings Using an Enhanced Particle Filter. IEEE Transactions on Instrumentation and Measurement*, vol. 64(10).

Li, T.C., Bolic, M. & Djuric, P.M. (2015), *Resampling Methods for Particle Filtering: Classification, implementation, and strategies. IEEE Signal Processing Magazine*, vol. 32 (3).

Antoni, J. (2007), *Cyclic spectral analysis in practice. Mechanical Systems and Signal Processing,* vol. 21(2), pp. 597-630.

Ricardo Mauricio A., Qi J. & Gryllias K. (2018), *Vibration based condition monitoring of wind turbine gearboxes based on cyclostationary analysis. ASME 2018 Turbomachinery Technical Conference Exposition.* June 11-15, Oslo, Norway.

Qiu, H., Lee, J., Lin, J. & Yu, G. (2006), *Wavelet filter-based weak signature detection method and its application on rolling element bearing prognostics. Journal of Sound and Vibration,* vol. 289(4–5), pp. 1066-1090.

BIOGRAPHIES

Junyu Qi received his B.S. and M.S. degree in Mechatronics from Shanghai Maritime University, Shanghai, China, in 2012 and from Friedrich-Alexander-University Erlangen-Nuremberg, Germany, in 2016, respectively. He is currently a PhD student in the Department of Mechanical Engineering of KU Leuven, Belgium. His research interests focus on condition monitoring of rotating machinery and particularly in prognostics.

Alexandre Mauricio received his MSc. degree in Mechanical Engineering from the Faculty of Engineering of the University of Porto (FEUP) in 2017. He is currently a PhD student at the Department of Mechanical Engineering of KU Leuven, Belgium. His main research interests focus on the diagnostics of rotating machinery operating under time varying conditions.

Mathieu Sarrazin holds a M.Sc. in Electromechanical-electrotechnical Engineering (2009) from the University of Gent Campus Kortrijk and a second M.Sc. in Mechanical Engineering, minor automotive (2012) from the KU Leuven. Since 2012, he is part of LMS International, now known as Siemens Industry Software (SISW). He has 6 years of experience in the applied research. In 2014, he received a unique Siemens Technology Award. Currently, he is a R&D manager and responsible for the definition, planning, managing and execution of research projects related to electro-mechanical drivetrains, model-based system testing, hybrid, electrical and autonomous vehicles, mechatronic systems, system identification, converter-machine interactions, control system strategies and condition monitoring.

Karl Janssens received his Engineer diploma (1995) and PhD degree (1999) from the Katholieke Universiteit Leuven, Belgium. In 2001, he joined LMS International, an engineering innovation company, developing advanced testing and simulation tools for mechatronic product design. LMS International became part of Siemens in 2013. He has more than 15 years of experience in the areas of rotating machinery testing, signal processing, noise source identification, transfer path analysis and sound engineering. At present, he is RTD Division Manager, responsible for research and technology innovation related to testing.

Konstantinos Gryllias holds a 5 years engineering diploma degree and a PhD degree in Mechanical Engineering from National Technical University of Athens, Greece. Since October 2014 he holds an assistant professor position on Vibro-acoustics of machines and transportation systems at the Department of Mechanical Engineering of KU Leuven, Belgium. He is also the manager of the University Core Lab Dynamics in Mechanical & Mechatronic Systems DMMS-M of Flanders Make, Belgium. His research interests lie in the fields of condition monitoring, signal processing, prognostics and health management of mech. & mechatronic systems.